Astron. Astrophys. 333, 1007–1015 (1998)

ASTRONOMY AND ASTROPHYSICS

An extensive ab initio study of the $C^+ + NH_3$ reaction and its relation to the HNC/HCN abundance ratio in interstellar clouds

D. Talbi[1] **and Eric Herbst**[2]

[1] Laboratoire d'Etude Theorique des Milieux Extrêmes, Ecole Normale Supérieure, 24 rue Lhomond, F-75005 Paris, France
[2] Departments of Physics and Astronomy, The Ohio State University, Columbus, OH 43210, USA

Received 18 July 1997 / Accepted 28 January 1998

Abstract. The hypothesis that the $C^+ + NH_3 \rightarrow CH_2N^+ + H$ reaction contributes to an HNC/HCN abundance ratio greater than unity in dark interstellar clouds has been tested using ab initio quantum chemical techniques. The hypothesis is based on the argument that a significant fraction of the ion product is the metastable H_2NC^+ isomer of C_{2V} geometry, rather than the linear $HNCH^+$ structure, and that the metastable isomer subsequently recombines with electrons to form HNC preferentially. Our extensive ab initio study of the ground and excited surfaces for the $C^+ + NH_3$ reaction shows, however, that this is most probably not the case. We find that the lowest energy path for reaction does lead initially to the formation of the metastable isomer in its ground singlet state, but that this product can then isomerize into the ground electronic state ($^1\Sigma^+$) of the linear $HCNH^+$ form. Dynamics calculations show that the isomerization destroys 97–98% of the product H_2NC^+ ion. We also follow excited potential energy surfaces which lead to the excited ($^3B_2$) electronic state of H_2NC^+, a state which does not interconvert to the linear ion. However, the potential energy surfaces exhibit barriers on the paths to formation of $H_2NC^+(^3B_2)$. We conclude that the H_2NC^+ isomer is a minor product of the $C^+ + NH_3 \rightarrow CH_2N^+ + H$ reaction.

Key words: ISM: abundances – ISM: molecules – molecular data – molecular processes

1. Introduction

Among the vexing problems in astrochemistry is the puzzling variability of the HNC/HCN abundance ratio in interstellar clouds, both from one source to another and even within one source. Although the metastable HNC is a fleeting rarity in the terrestrial laboratory, its abundance is significant in dense interstellar clouds. Indeed, the HNC/HCN abundance ratio can exceed unity in cold dark clouds (Irvine & Schloerb 1984; Irvine et al. 1987; Pratap et al. 1997). In OMC-1, a region of high mass star formation, the abundance ratio changes drastically from 1/80 in the immediate vicinity of Orion-KL to $\approx 1/5$ in adjacent ridge positions (Schilke et al. 1992; see also Ungerechts et al. 1997). All these observations indicate a variation of the abundance ratio with temperature. Their explanation would appear to require a production mechanism which has the capability of producing more HNC than HCN and a destruction mechanism which preferentially destroys the higher energy (HNC) form as the temperature rises.

Although the formation and destruction of both HCN and HNC in current gas-phase interstellar models (Pineau des Forêts et al. 1990; Lee et al. 1996; Millar et al. 1997) is thought to involve a variety of processes, a major contributor to the formation of the former and the latter is the reaction $C^+ + NH_3 \rightarrow CH_2N^+ + H$, where we have written the product ion in a manner which does not denote its structure. Although the reaction has been studied in the laboratory (Marquette et al. 1985), the precise nature of the ion product has not been determined. It undoubtedly consists of the two known isomeric structures – the lower energy linear form – $HCNH^+$ – and the higher energy H_2NC^+ structure:

$$C^+(X^2P) + NH_3 \rightarrow \begin{cases} HCNH^+ + H & (1a) \\ H_2NC^+ + H & (1b) \end{cases}$$

Once these ions are produced via reaction (1) and by other lesser processes ($C + NH_3^+$ and $N + CH_3^+$), the product ions are thought to dissociatively recombine to form the HNC and HCN neutrals:

$$HCNH^+ + e^- \rightarrow \begin{cases} HCN + H & (2a) \\ HNC + H & (2b) \end{cases}$$

$$H_2NC^+ + e^- \rightarrow HNC + H\ . \quad (3)$$

Other channels, both neutral-neutral and ion-molecule, exist for the production of HCN and HNC (Pineau des Forêts et al. 1990). In addition to ion-controlled depletion processes, which are unlikely to distinguish strongly between the two isomers, the following neutral-neutral reactions may play a role in the selective destruction of HNC:

$$HNC + H \rightarrow HCN + H \quad (4)$$

$$HNC + O \rightarrow NH + CO\ . \quad (5)$$

To help reproduce observed abundances for HCN and HNC, some assumptions about processes (1)–(5) have been made in astrochemical models. To account for the high (≥ 1) HNC/HCN abundance ratio in cold dark clouds, it is normally assumed that:

1) process (1b) is at least as important as (1a) and preferably more so, despite the metastable nature of the product ion,
2) process (3) leads only to HNC,
3) the HNC/HCN product ratio is 1 from reactions (2a) and (2b),
4) reactions (4) and (5) are inefficient because of activation energies.

To account for the relatively low HNC/HCN abundance ratio in warmer clouds, it is also assumed that:

5) reactions (4) and (5) become relevant at higher temperatures, adding to the HNC destruction rate.

With assumptions 1–4, the current UMIST network (Millar et al. 1997) is able to produce an HNC/HCN abundance ratio greater than unity for old and cold dark clouds. In particular, reaction (1) is assumed to produce only the H_2NC^+ ion. The models of Lee et al. (1996) do not obtain an HNC/HCN abundance ratio greater than unity since they contain the assumption that (1a) and (1b) are of equal probability. All these assumptions, if very appealing, have never been confirmed through laboratory experiments because accurate experiments in this field are extremely hard to realize. For that reason we have embarked on a program of ab initio quantum chemical calculations to determine the potential energy surfaces of these reactions. These energy surfaces are crucial for an understanding of the reaction mechanisms and a determination of the efficiency of the chemical processes.

In a previous calculation (Talbi et al. 1996) of the potential energy surface of reaction (4), we showed because the activation energy for the process is four times smaller than for the reverse endothermic path starting with the reactants HCN + H, there is a domain of temperatures where the direct reaction consumes HNC while the reverse one is still inhibited. However, our rate coefficient calculations suggest that this reaction is still not efficient enough at consuming HNC, unless the effective temperature of the interstellar regions where HNC/HCN is small is in excess of 300 K, which is higher than customarily estimated.

In a second theoretical study, we have confirmed the suggestion that reaction (2) does lead to equal amounts of HNC and HCN (Talbi and Ellinger 1998). Using sophisticated methods of quantum chemistry which allow an equally balanced treatment for reactions (2a) and (2b), we have shown that the lowest dissociative surfaces leading respectively to HCN + H and HNC + H cross the potential curve of the ion at its minimum, allowing efficient "direct" curve-crossing from the stable ionic surface to the repulsive neutral surfaces. The same conclusion has been drawn for the indirect process, for which we have shown that the crossing between dissociative and Rydberg states is at the same energy level for both dissociation channels.

In this paper, we report a detailed study of reaction (1), with special emphasis on the nature of the products and how they can be produced from reactants. Some work related to this reaction has already been published. In particular, Allen et al. (1980) and DeFrees et al. (1986) have investigated the singlet and triplet structure of H_2NC^+as well as the potential energy surface for the H_2NC^+/$HCNH^+$ interconversion. Among the C^+ (^{2}P) + NH_3 possible reaction products, H_2NC^+ in its ground ($^1A_1$) electronic state is a very appealing one since it will lead to preferential formation of HNC through dissociative recombination (reaction 3). The work of Allen et al. (1980) has shown that the production of H_2NC^+ ($^1A_1$) is strongly exothermic but it also has suggested that the barrier to subsequent isomerization of this ion into the lower energy ion $HCNH^+$ in its ground $^1\Sigma^+$ electronic state is too low to prevent isomerization from occurring. The suggestion that most if not all H_2NC^+($^1A_1$) undergoes subsequent isomerization is perhaps too facile since a detailed analysis of the isomerization rates in both directions was not undertaken. Such an analysis will be reported in this paper. A second possible route to the production of HNC without simultaneously forming HCN was proposed by Allen et al. (1980) who suggested that H_2NC^+ product in its excited $^3B_2$ electronic state might play a role in the formation of H_2NC^+ ($^1A_1$) if, after formation, phosphorescence from the excited state stabilizes the system in a low-lying vibrational state where the singlet H_2NC^+ isomer has insufficient energy to isomerize to $HCNH^+$ ($^1\Sigma^+$). It would remain in this structure until dissociative recombination occurs through reaction (3), thus producing HNC without HCN.

Despite the previous work, there is, to the best of our knowledge, no previous detailed study of the potential energy surfaces for the formation of H_2NC^+($^1A_1$) and H_2NC^+($^3B_2$) from C^+(^{2}P) + NH_3. Because it is crucial for an understanding of the HNC/HCN abundance ratio in interstellar clouds to determine the branching fractions of the CH_2N^+ isomers in reaction (1), we have decided to investigate these potential energy surfaces using ab initio methods of quantum chemistry.

A first insight as to how C^+ and NH_3 (as well as $C + NH_3^+$) connects with the different products can be obtained from the correlation diagram shown in Fig. 1. All structures shown in the figure have been optimized and corrected for the zero-point energies (Table 1). The methods used and calculation protocols are discussed in the Appendix. On the right-hand side are shown the C(^{3}P) + NH_3^+ and C^+(^{2}P) + NH_3 reactants; on the left-hand side are shown the final products CH_2N^+ + H. In between these two limits, intermediate H_3NC^+ structures in assorted states are shown. In the C_s plane of symmetry, defined in Fig. 2, the lowest A′ and A″ H_3NC^+ stable structures are the two components of the lowest H_3NC^+(^{2}E) complex which is formed when carbon approaches ammonia along its C_{3v} axis. Calculated in the lower C_s symmetry, the 1^2A′ and 1^2A″ components have slightly different energies (see Table 1) because of the so-called Jahn-Teller distortion. However, these states are effectively degenerate since the calculated energy separation is less than 0.1 kcal/mol (1 kcal/mol = 503 K). Whether a weak Jahn-Teller effect exists or not is of limited importance for the present study. The energy splitting of the A′ and A″ components

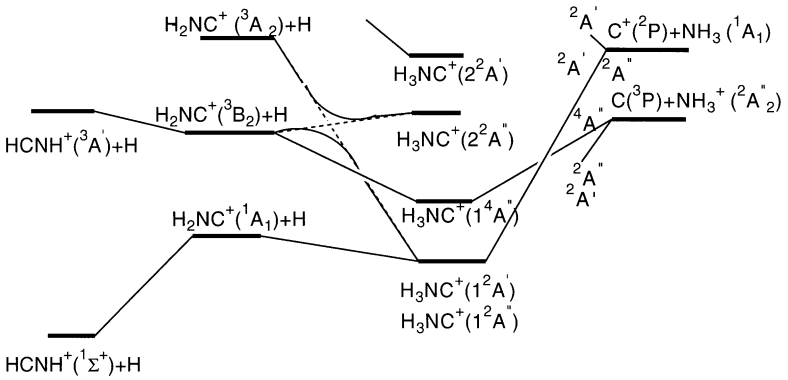

Fig. 1. Correlation diagram established at the MP2/6-31G(d,p) level using geometries optimized at the same theoretical level. Scaled zero point energies are taken in account

Table 1. MP2/6-31G(d,p) absolute energies

Molecule	State	E	e_0
H	^{2}S	− 0.498232	–
C^+	^{2}P	−37.331066	–
C	^{3}p	−37.736506	–
NH_3	$^1A_1$	−56.386919	0.034405
NH_3^+	$^2A_2''$	−56.032323	0.032841
H_3NC^+	$1^2A'$	−93.902484	0.037025
H_3NC^+	$1^2A''$	−93.902533	0.038212
H_3NC^+	$1^4A''$	−93.860341	0.041321
H_3NC^+	$2^2A''$	−93.774640	0.038776
H_3NC^+	$2^2A'$	−93.720810	0.038034
$HCNH^+$	$^1\Sigma^+$	−93.457297	0.026877
H_2NC^+	$^1A_1$	−93.365765	0.025252
H_2NC^+	$^3B_2$	−93.279118	0.028159
$HCNH^+$cis	$^3A'$	−93.262376	0.024754
$HCNH^+$trans	$^3A'$	−93.248453	0.023250
H_2NC^+	$^3A_2$	−93.202224	0.025373

Energies in Hartrees, are calculated for MP2/6-31G(d,p) optimized geometries e_0 in Hartrees, are MP2/6-31G(d,p) zero-point vibrational energies scaled by 0.969. 1 Hartree = 27.21 eV

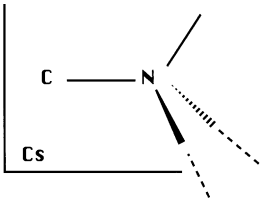

Fig. 2. Definition of the symmetry plane used in the calculations. Plane including the C,N,H atoms and bissecting the plane of the two other hydrogens

is negligible compared with the relative energies involved in the processes and therefore can be ignored.

The correlation diagram shows that both the lowest $^2A'$ and $^2A''$ states of H_3NC^+correlate with C(^{3}P) + NH_3^+, which lies lower in energy than C^+(^{2}P) + NH_3. However, the C(^{3}P) + NH_3^+ entrance channel, apparently more appealing for energetical reasons, is of less importance in chemical models (Lee et al. 1996) than reaction (1). The two lowest states of H_3NC^+ can be reached from C^+(^{2}P) + NH_3 reactants because charge transfer can occur at long range distances: as the reactants approach each other, the $[C...NH_3]^+$ common entity will stabilize to H_3NC^+ via vibronic coupling through the umbrella mode of the NH_3/NH_3^+ fragments.

Within the C_s plane (Fig. 2), H_3NC^+ $1^2A'$ adiabatically correlates with H_2NC^+ ($^1A_1$) which may isomerize to the lower energy $HCNH^+$ ($^1\Sigma^+$) given sufficient internal energy (there is a barrier not shown in Fig. 1) while H_3NC^+ ($1^2A''$) correlates with H_2NC^+ ($^3B_2$), which is more stable than the corresponding triplet state of the $HCNH^+$ arrangement. There is a complication with the latter correlation: the direct (diabatic; dotted line) correlation leads to the second ($^3A_2$) excited triplet state H_2NC^+ rather than the first ($^3B_2$) excited state. However, there is a so-called "avoided" crossing between the $1^2A''$ and the $2^2A''$ states of H_3NC^+ so that the $1^2A''$ state can indeed correlate adiabatically with H_2NC^+ ($^3B_2$), but with the possible existence (confirmed below) of a barrier on this part of the surface. In this and subsequent discussions, the structure corresponding to a potential barrier, or saddle point, will be referred to as a transition state. There is another possible pathway which leads to H_2NC^+ ($^3B_2$) but only from the C(^{3}P) + NH_3^+ reactants, since these can form quartet as well as doublet states. In this pathway, the reactants correlate with the excited $1^4A''$ state of H_3NC^+ which in turn leads to the $^3B_2$ state of H_2NC^+.

The remainder of the paper is organized as follows. In Sects. 2 and 3 we present the detailed formation of the assorted product and product states of reaction (1), while in Sect. 4, we demonstrate that isomerization of the ground state of H_2NC^+ into the ground state of $HCNH^+$ is rapid and efficient. In Sect. 5, we discuss our conclusions. Our methodology for the quantum chemical calculations and related technical details are presented in the appendix.

2. The formation of H_2NC^+ ($^1A_1$) and $HCNH^+$ ($^1\Sigma^+$)

For the stationary points on the C^+(^{2}P) + $NH_3 \rightarrow H_2NC^+$($^1A_1$) + H $\rightarrow$ $HCNH^+$ ($^1\Sigma^+$) + H potential energy surface, the absolute and relative energies, corrected for zero-point vibrational energies, are given in Table 2, while the molecular structures and the energy profile of the reaction path are depicted Fig. 3 and Fig. 4, respectively (see appendix for computational details). From Fig. 4, one can see that there is no long-range barrier on the portion of the potential energy surface leading

Table 2. Absolute and relative energies calculated at the MP4SDTQ/6-311 + + G(3df,3pd) level for the lowest $2A'$ surface

Molecule	E_0	$\Delta E^{(1)}O$	$\Delta E^{(2)}O$
$C(^2P)^+ + NH_3(^1A_1)$	−93.84964	0.0	0.0
$H_3NC^+(^2A')$	−94.02514	−110.	−110.
$(H_3NC^+)_{ts}(^2A')$	−93.95950	−68.9	−69.
$H_2NC^+(^1A_1) + H$	−93.99365	−90.4	−90.5
$(H_2NC^+)_{ts}(^1A') + H$	−93.96510	−72.5	−72.4
$HCNH^+(^1\Sigma^+) + H$	−94.08017	−145.	−145.

E_0, energies in Hartrees, are calculated using $MP3/6-311++G(d,p)$ optimized geometries; they are corrected for scaled zero point energies. At this theoretical level, E_0 is −56.09409 Hartrees for $NH3^+(^2A_2'')$ and −37.79639 Hartrees for $C(^3P)$. ΔE_o are relative energies in Kcal/mol corrected for scaled zero point energies. (1) relative energies calculated using MP3/6-311 + + G(d,p) optimized geometries (2) relative energies calculated using MP2/6-31G(d,p) optimized geometries. Negative energies are for exothermic balances. Structures and geometries are shown in Fig. 3. 1 Hartree = 27.21 eV

from reactants to the $1^2A'$ component of $H_3NC^+(X^2E)$. The reaction path to $H_2NC^+(^1A_1)$ is obtained through the in-plane stretch of one of the NH bonds. Once formed, $H_2NC^+(^1A_1)$ can isomerize to a more stable linear geometry (Fig. 4) by going over a transition state $(H_2NC^+)_{ts}$. The transition state nature of $(H_3NC^+)_{ts}$ with respect to dissociation to $H_2NC^+(^1A_1)$ + H and of $(H_2NC^+)_{ts}$with respect to isomerisation into $HCNH^+$ is confirmed by the vibrational analysis in Table 3.

From the energy profile of Fig. 4, it is obvious that the transition structures $(H_3NC^+)_{ts}$ and $(H_2NC^{+)}_{ts}$ lie much lower in energy than the initial reactants, (68.9 and 72.5 kcal/mol below reactants, respectively). It is therefore clear that the vibrationally excited $[H_3NC^+]$ complex (energy minimum) formed by the collision will easily overcome the corresponding barrier opposing the formation of H_2NC^+ ($^1A_1$) + H. The subsequent isomerization to linear $HCNH^+(^1\Sigma^+)$ is a more complex problem since it depends on the amount of relative translational energy between H_2NC^+ ($^1A_1$) + H, as well as on other matters. This isomerization will be discussed in Sect. 4.

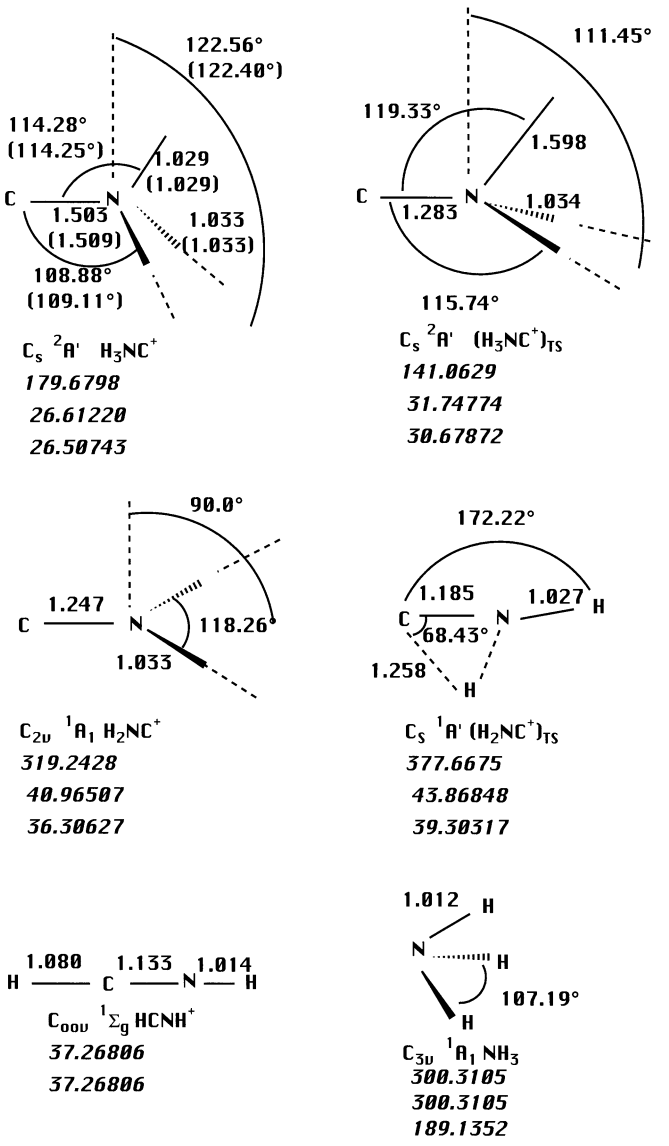

Fig. 3. MP3/6-311 + + G(d,p) stable and transition structures along the $1\,^2A'$ H_3NC^+ surface. For $H_3NC^+(^2A')$ are also reported the MP2/6-31G(d,p) optimized geometries (between brackets) for comparison. Italic numbers correspond to the rotational constants (in Ghz) calculated at the MP3/6-311 + + G(d,p) energy level. Bond lengths are in Angstroms and angles in degrees.

3. The formation of H_2NC^+ ($^3B_2$)

3.1. Formation through the doublet surface

The energy profile, or potential energy surface, for the $C^+(^2P)$ + $NH_3 \rightarrow H_2NC^+(^3B_2)$ + H reaction is given in Fig. 5, the corresponding relative energies of the stationary points, corrected for zero-point energies and spin contaminations from higher spin states (see appendix) are gathered in Table 4, and the molecular structures of the stationary points presented in Fig. 6. In the C_s symmetry plane defined previously, this potential surface has A'' symmetry. Looking at Fig. 5, we see that the stable $H_3NC^+(1^2A'')$ complex is formed without any potential barrier but, as in the ground state potential surface, has to proceed through a transition state $(H_3NC^{+)}_{ts}$ before dissociation to H_2NC^+ ($^3B_2$) + H. The nature of the transition state with respect to dissociation to $H_2NC^+(^3B_2)$ + H is confirmed by the vibrational analysis shown in Table 3. This transition state is calculated to lie higher in energy than the reactants $C^+(^2P)$ + NH_3 by 6.5 kcal/mol. As a consequence, even though the $C^+(^2P)$ + $NH_3 \rightarrow H_2NC^+$ ($^3B_2$) + H reaction is exothermic by 32.3 kcal/mol, the barrier height of 6.5 kcal/mol will reduce the reaction to a minor process exept possibly at very high temperatures.

The endothermic isomerization of H_2NC^+ ($^3B_2$) to $HCNH^+$ *cis* ($^3A'$) has not been considered in the present study. This process, which is of little interest for the present problem, has been extensively investigated by DeFrees et al. (1986), who found a barrier of 63 kcal/mol.

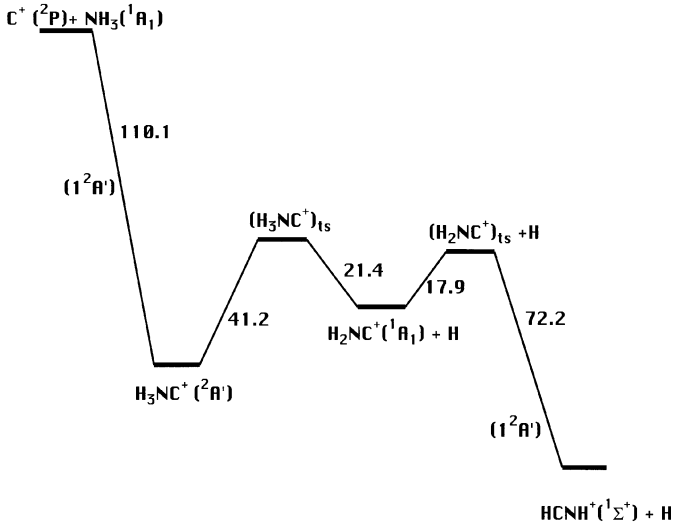

Fig. 4. Energy profile (in Kcal/mol) for the $C^+(^2P) + NH_3 \rightarrow H_2NC^+(^1A_1) + H \rightarrow HCNH^+(^1S^+) + H$ reaction, calculated at the MP4SDTQ/6-311 + + G(3df,3pd) using MP3/6-311 + + G(d,p) optimized geometries. Scaled zero point energies are taken in account.

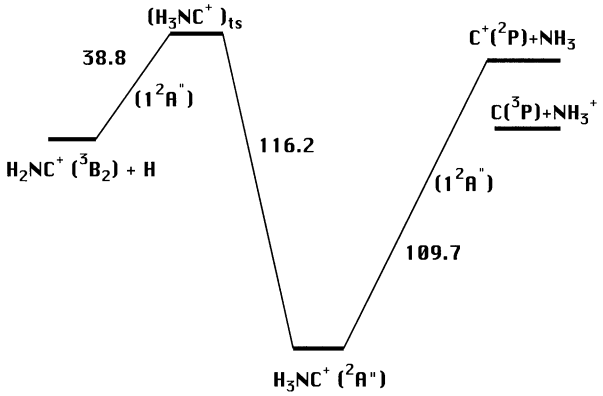

Fig. 5. Energy profile (in Kcal/mol) for the $C^+(^2P) + NH_3 \rightarrow H_2NC^+(^3B_2) + H$ reaction, calculated at the MP4SDTQ/6-311 + + G(3df,3pd) using MP2/6-31G(d,p) optimized geometries. Scaled zero point energies and spin contamination effects are taken in account.

3.2. Formation through the Quartet surface

The energy profile for the $C(^3P) + NH_3^+(^2A''_2) \rightarrow H_2NC^+(^3B_2) + H$ reaction, is shown in Fig. 7. The corresponding relative energies, corrected for zero-point vibrational energies and spin contamination effects, can be found in Table 4 while the molecular structures are in Fig. 6. In C_s symmetry, this potential surface, of quartet multiplicity, also belongs to the A″ representation. As in the previous case, although the entrance channel corresponding to $C(^3P)$ approaching NH_3^+ is very attractive, there is a barrier to overcome for the stable $H_3NC^+(^4A'')$ to dissociate to $H_2NC^+(^3B_2)$ + H. The $(H_3NC^+)_{ts}$ $(^4A'')$ transition state (see Table 3 for the vibrational analysis) lies 2.9 kcal/mol above the $C(^3P) + NH_3^+$ reactants. Considering the relatively low abundances of C and NH_3^+ in dark clouds and the existence of a barrier on the potential energy path, the formation of the H_2NC^+ $(^3B_2)$ through the quartet surface can be considered as an inefficient process.

Table 3. MP2/6-31G(d,p) harmonic vibrational frequencies

Molecule	Frequencies
H_3NC^+	a′ = 812, 982, 1488, 1628, 3351, 3492
$(^2A')$	a″ = 613i, 1590, 3428
H_3NC^+	a′ = 752, 885, 1487, 1653, 3341, 3452
$(^2A'')$	a″ = 713, 1533, 3492
H_3NC^+	a′ = 1123, 1140, 1568, 1678, 3400, 3503
$(^4A'')$	a″ = 1123, 1678, 3503
$(H_3NC^+)_{ts}$	a′ = 2439i, 735, 1068, 1413, 1625, 3350
$(^2A')$	a″ = 640, 964, 3441
$(H_3NC^+)_{ts}$	a′ = 4108i, 275, 715, 1283, 1625, 3407
$(^2A'')$	a″ = 470, 1285, 3552
$(H_3NC^+)_{ts}$	a′ = 1506i, 643, 1082, 1573, 1693, 3463
$(^4A'')$	a″ = 812, 1199, 3578
H_2NC^+	a_1 = 1413, 1779, 3373
$(^1A_1)$	b_2 = 634, 3469
	b_1 = 771
H_2NC^+	a_1 = 1652, 1923, 3474
$(^3B_2)$	b_2 = 1179, 3594
	b_1 = 934
$(H_2NC^+)_{ts}$	a′ = 1483i, 917, 1991, 2395, 3499
$(^1A')$	a″ = 595
$HCNH^+$	σ_g = 2161, 3404, 3693
$(^1\Sigma^+)$	π_i = 635, 824
NH_3	a_1 = 1120, 3565
$(^1A_1)$	e = 1728, 3722
NH_3^+	a'_1 = 3460
$(^2A''_2)$	e′ = 1598, 3670
	a''_2 = 882

Frequencies are given in cm^{-1}. They have to be scaled by 0.969 before use. See Fig. 3. for structures of A′ symmetry and Fig. 6. for structures of A″ symmetry

4. Isomerization of $H_2NC^+(^1A_1)$ into $HCNH^+(^1\Sigma^+)$

Given the barrier calculated for formation of H_2NC^+ in its excited $^3B_2$ state from $C^+ + NH_3$ reactants, the only possibility for production of this metastable ion via reaction (1) would appear to lie in the stabilization of ground state H_2NC^+, which is formed as a primary product by the reaction occurring on the ground potential surface (Figs. 1 and 4). Although there is formally enough total energy for isomerization of H_2NC^+ into $HCNH^+$ (Fig. 4) over the H_2NC^+ transition state, there are several reasons that isomerization need not be rapid or even occur at all. First, the exothermicity of reaction may go sufficiently into relative translation between H_2NC^+ and H that there is not enough internal energy left in H_2NC^+ for it to overcome the transition state barrier. Secondly, there is a large amount of angular momentum in ion-polar molecule collisions and this angular momentum, if converted into rotational angular mo-

Table 4. Relative energies calculated at the MP4SDTQ/6-311 + + G(3df,3pd) level for the lowest $^2A''$ and $^4A''$ surfaces

Molecule	$\Delta E_0^{(1)}$	$\Delta E_0^{(2)}$
$C^+(^2P) + NH_3(^1A1)$	0.0	
$C(^3P) + NH_3^+(^2A_2'')$		0.0
$H_3NC^+(^2A'')$	−110.	
$H_3NC^+(^4A'')$		−45.2
$(H_3NC^+)_{ts}$ $(^2A'')$	+ 6.5	
$(H_3NC^+)_{ts}(^4A'')$		+ 2.9
$H_2NC^+(^3B_2) + H$	−32.3	−5.7

ΔE_o are relative energies in Kcal/mol calculated for MP2/6-31G(d,p) optimized geometries. They are corrected for scaled zero point energies and spin contamination from higher spin states. $\Delta E_0^{(1)}$: energies relative to the $C^+(^2P) + NH_3(^1A1)$ limit for the A'' surface. $\Delta E_0^{(2)}$: energies relative to the $C(^3P) + NH_3^+(^2A_2'')$ limit for the A'' surface. Negative energies are for exothermic balances. Structures and geometries can be found Fig. 6. 1 Hartree = 27.21 eV.

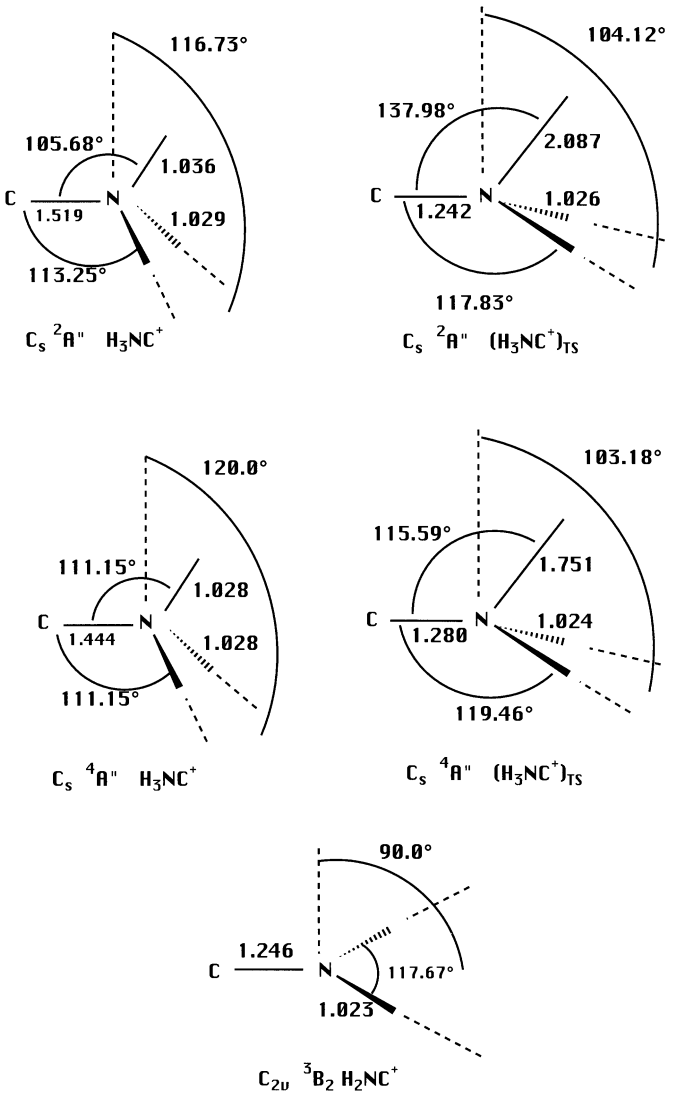

Fig. 6. MP2/6-31G(d,p) stable and transition structures along the 1 $^2A''$ and 1 $^4A''$ H_3NC^+ surfaces. Bond lengths are in Angstroms and angles in degrees.

mentum of the H_2NC^+ product, rather than into relative angular momentum of the two products, effectively slows the rate of isomerization since only vibrational energy is useful in this process (Herbst 1996). Thirdly, relaxation of the ground state H_2NC^+ ion product via emission of infrared radiation (and, in the laboratory, by collision) to vibrational-rotational states below the barrier to isomerization may be more rapid than isomerization. For these three reasons, it is necessary to estimate the rate of isomerization and then determine the fraction of product that can remain as H_2NC^+.

Our first consideration is to estimate how much energy goes into relative translation between the products. Although both statistical theories and assorted experiments (Illies et al. 1983) show that the energy of exothermic reactions tends to wind up as vibrational energy in polyatomic products, experiments also show that in the case of potential surfaces with barriers, a significant amount of translational energy, with a distribution centered on the potential energy difference between transition state and products, can be released (Jarrold et al. 1986). Reference to Fig. 4 shows that the transition state between the H_3NC^+ energy minimum and the H_2NC^+ $(^1A_1)$ + H products lies at an energy of 21.4 kcal/mol above the reactants. It is most likely that the separating products carry away this much translational energy, leaving the remainder of the reaction exothermicity of H_2NC^+ $(^1A_1)$ + H products $(110.1 - 41.2 = 68.9$ kcal/mol) as vibrational-rotational energy of H_2NC^+ $(^1A_1)$. Since the transition state energy for isomerization of this ion into the lower energy $HCNH^+$ ion is only 17.9 kcal/mol (see Fig. 4), the H_2NC^+ ion possesses sufficient internal energy to isomerize as long as its vibrational energy exceeds 17.9 kcal/mol. To have less vibrational energy than this, the ion must relax rapidly or have large amounts of angular momentum. Both possibilities are addressed below.

The rate of isomerization over a barrier can be treated by the RRKM statistical method (Herbst 1996). In this formulation, the rate $k(s^{-1})$ as a function of vibrational-rotational energy E and angular momentum quantum number J is given by the expression

$$k(E, J) = N^+(E - \varepsilon - E_{rot}(J))/[h\rho\,(E - E_{rot}(J))] \qquad (I)$$

where h is Planck's constant, N^+ refers to the total number of vibrational states of the transition state from its minimum allowable energy ε through $E - E_{rot}(J)$, and ρ refers to the density of vibrational states of the H_2NC^+ isomer at energy $E - E_{rot}(J)$. Note that $\varepsilon = 17.9$ kcal/mol is the energy difference between H_2NC^+ and the transition state. The rotational energy $E_{rot}(J)$ for either the ion or transition state can be approximated as that of a spherical top with one rotational constant B equal to the geometric mean (cube root) of the product of three rotational constants. For both the number of states of the transition state and the density of states of the complex, the semi-classical expression of Whitten and Rabinovitch (1964) can be used.

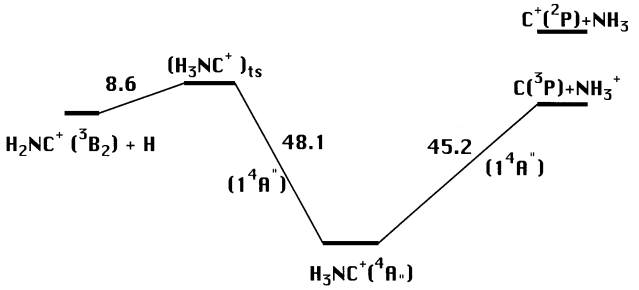

Fig. 7. Energy profile (in Kcal/mol) for the $C(^3P) + NH_3^+ \rightarrow H_2NC^+(^3B_2) + H$ reaction (surface of quartet multiplicity), calculated at the MP4SDTQ/6-311 + + G(3df,3pd) using MP2/6-31G(d,p) optimized geometries. Scaled zero point energies and spin contamination effects are taken in account.

With our calculated energies as well as the vibrational frequencies (Table 3) and rotational constants of the H_2NC^+ ion and transition state (see Fig. 3), we can determine k(E,J). Using the assumption that 21.4 kcal/mol of reaction energy goes into relative translational energy and is thus not available for isomerization of H_2NC^+, we still determine that isomerization is very rapid for a wide range of angular momenta and vibrational energies. Let us consider two extreme cases: when the ion possesses no angular momentum (J = 0) and when it possesses a large angular momentum, quantum number J = 78, which is the maximum quantum number for which there is sufficient vibrational energy for isomerization to occur. For the former case, we calculate that the isomerization rate for H_2NC^+ into $HCNH^+$ before any vibrational relaxation can occur is $\approx 1 \times 10^{13}\,s^{-1}$ while the equivalent rate after sufficient vibrational relaxation such that H_2NC^+ can just overcome the transition state barrier is $\approx 1 \times 10^{11}\,s^{-1}$. For the latter case, we calculate the isomerization rate to be $\approx 5 \times 10^{10}\,s^{-1}$ (vibrational relaxation in this case will prevent isomerization). Consideration of tunneling under the transition state barrier (Herbst 1996) will enlarge these already large values. We conclude that isomerization is a rapid process for all allowable J; in particular, it is much more rapid than radiative relaxation, which is known to occur at a rate of only 10–$10^3\,s^{-1}$ for vibrational states (Herbst 1982; Herbst & Dunbar 1991). Thus we are led to the following picture: after the H_2NC^+ ion is formed in its ground electronic state, it will rapidly isomerize to the $HCNH^+$ ion for angular momenta from J = 0 to a maximum value, and, as can be shown by calculations similar to the above, this ion will rapidly isomerize in the backwards direction so that an equilibrium will quickly be achieved between the two ions. As the ions slowly relax vibrationally, the equilibrium will reflect the change in energy. The relevant equilibrium for our purposes will be that corresponding to a vibrational energy just equal to the transition state barrier. A similar analysis was performed previously by De Frees et al. (1985) for the $CH_3CNH^+ - CH_3NCH^+$ isomerization.

To determine the equilibrium populations of ground state H_2NC^+ and $HCNH^+$, it is necessary to calculate the so-called equilibrium coefficient K, which is related to the ratio of the forward and backward rates of isomerization. The equilibrium coefficient in the microcanonical formulation is given by the equation

$$\mathrm{K(E,J)} = \rho^{\mathrm{L}}\left(E - E_{\mathrm{rot}}(J)\right)(2J+1) \Big/ \left[\rho^{\mathrm{NL}}\left(E + E_{\mathrm{diff}} - E_{\mathrm{rot}}(J)\right)(2J+1)^2/2\right] \quad \text{(II)}$$

where ρ once again refers to the vibrational density of states, the subscripts L and NL refer to the linear and non-linear isomers, respectively, and E_{diff} refers to the (positive) difference in energy between the two isomers. Part of this expression can be obtained by dividing the RRKM rate equations for the forward process by that for the backward process since the two processes possess the same transition state. But, one must also consider the rotational degeneracies of the two isomers, which are 2J + 1 for the linear ion and $(2J + 1)^2$ for the non-linear ion (assumed to be a spherical top). In addition, there is a symmetry factor $\sigma = 2$ for the two-fold symmetry of the non-linear ion. Expression (II) should be evaluated for vibrational energies corresponding to the energy of the transition state. Restricting attention to the energy at the barrier height, and using the Whitten-Rabinovitch (1964) density-of-states formulation, we obtain that K(J) = 3168/(2J + 1) for all values of J for which a sufficient amount of vibrational energy can be obtained. For values of $J > J_{max}$, where J_{max} is determined by the amount of relative translational energy, a sufficient amount of vibrational energy cannot be obtained, and K(J) = 0. For our standard choice of translational energy, $J_{max} = 78$.

The rotationally-averaged equilibrium coefficient K is obtained from the formula

$$\mathrm{K} = \Sigma\, \mathrm{p(J)K(J)} \quad \text{(III)}$$

where p(J) is the probability that the reaction produces H_2NC^+ in a specific rotational level of angular momentum quantum number J. This probability can be estimated by the statistical relation (Herbst 1996)

$$\mathrm{p(J)} = \mathrm{N}(2\mathrm{J}+1)^2 \rho^{\mathrm{NL}}\left(\mathrm{E} - \mathrm{E_{rot}(J)}\right) \quad \text{(IV)}$$

where N is a normalization coefficient. Eq. (IV) holds for values of J from 0 to a maximum $J'_{max} > J_{max}$ defined by the stronger of several constraints posed by the details of the reaction and by conservation of energy. If J'_{max} is sufficiently large, then the averaged equilibrium constant can be small, so that isomerization need not destroy a large amount of H_2NC^+. After doing the rotational averaging, however, we find that K = 44 if the relative product translational energy is set at 21.4 kcal/mol (our preferrred value), and K = 39 if the relative translational energy is set at 0. The weak dependence on translational energy means that this parameter is not of the utmost importance. Since the equilibrium coefficient tells us the ratio of the population of $HCNH^+$ product to H_2NC^+ product, we conclude that the amount of the latter is only about 2–3% of the total and that $HCNH^+$ is the overwhelmingly dominant product for reaction (1) when it occurs on the lowest energy potential surface.

5. Conclusion

The ab initio quantum chemical and dynamical calculations reported here provide a crucial test of the present astrochemical

assumption that reaction (1) produces a significant fraction of product channel (1b), namely $H_2NC^+ + H$. This assumption is one route for models to reproduce the observed greater-than-unity HNC/HCN abundance ratio in cold dark clouds, because the metastable H_2NC^+ isomer subsequently leads to only the metastable neutral isomer HNC via dissociative recombination with electrons. Channel (1a), on the other hand, produces the linear ion $HCNH^+ + H$, and the linear ion has long been thought to dissociatively recombine to both HNC and HCN with equal probability (Watson 1976), a position strongly reinforced by our recent calculations (Talbi & Ellinger 1998). Contrary to the presently accepted picture, however, we have found that reaction (1) leads mainly to product channel (1a), namely $HCNH^+ + H$. There are two main reasons for our finding. First, when the reaction proceeds along the lowest potential energy surface, it leads directly to metastable H_2NC^+ in its lowest electronic state. Although there is a barrier for subsequent isomerization into the lowest electronic state of $HCNH^+$, our detailed dynamical calculations show that only 2–3 percent of the ground state H_2NC^+ product manages to avoid being converted into the linear ion. Secondly, the potential surface leading to the first excited ($^3B_2$) state of H_2NC^+ has a significant potential barrier so that low energy $C^+ + NH_3$ collisions cannot possibly lead to this state as a product. Starting from the reactants $C + NH_3^+$, there is a second pathway to production of H_2NC^+ in its $^3B_2$ electronic state; this involves a potential energy surface of quartet multiplicity. However, like the other pathway, this one also involves a potential energy barrier. Production of the H_2NC^+ ion in any electronic state thus seems to be unlikely for both the $C^+ + NH_3$ and $C + NH_3^+$ reactants. This theoretical result should be confirmed by laboratory reactivity studies on the ion product of reaction (1). Since laboratory studies are undertaken at higher densities than the interstellar environment, however, the results may have to be interpreted carefully. For example, it is possible, but not likely, that the H_2NC^+ ion produced in the laboratory can be stabilized via collisions before isomerization into the more stable linear form.

Are there other significant ion-molecule pathways leading to the metastable H_2NC^+ ion? In work yet to be reported (Talbi 1998), we have shown that another important reaction in interstellar clouds:

$$N + CH_3^+ \rightarrow CH_2N^+ + H \quad (6)$$

also leads to the linear $HCNH^+$ ion. It would thus appear that an HNC/HCN abundance ratio greater than unity in cold interstellar clouds cannot be explained by ion-molecule formation reactions. It is also unlikely but not impossible that any destruction channels, be they ion-molecule or neutral-neutral, would be slower for the metastable HNC than for the stable HCN. Past research, including our own, has, on the contrary, looked at selective destruction reactions for HNC (processes (4) and (5)) to explain its lower abundance at higher temperatures.

To explain the low temperature HNC/HCN abundance ratio, we are left with the hypothesis of an additional neutral-neutral reaction pathway for HNC which must be more rapid than an analogous pathway for HCN. It would be even nicer if this hypothetical neutral-neutral pathway were only rapid at low temperature. Current reaction networks (Millar et al. 1997; Lee et al. 1996) do include neutral-neutral reactions such as:

$$C + NH_2 \rightarrow HNC + H \quad (7)$$

$$N + CH_2 \rightarrow HCN + H \quad (8)$$

although the rate coefficients are highly uncertain for a variety of reasons. If reaction (7) were very rapid at low temperatures, perhaps the low temperature HNC/HCN riddle would be at least partially solved.

But, even if neutral-neutral chemistry can explain the low temperature problem, we must still account for the high temperature problem by either finding additional depletion reactions for HNC or additional formation mechanisms for HCN. Work on the HNC + H reaction (process 4) has shown that this reaction cannot explain the decrease in HNC abundance in warm clouds below 300 K (Talbi et al. 1996). Work on HNC + O (process 5) is in progress and shows, to date, a rather high potential barrier, which would also indicate its inability to selectively deplete HNC at warm temperatures in the 100–300 K range.

In summary, despite many years of theoretical work and detailed interstellar models, it appears that we are still far removed from a complete understanding of the temperature dependence of the HNC/HCN abundance ratio in dense interstellar clouds.

Acknowledgements. Part of the calculations reported in this paper were supported by the "Institut du Développement et des Ressources en Informatique Scientifique" (IDRIS) which is gratefully acknowledged. E.H. acknowledges the support of the National Science Foundation for his research program in astrochemistry. He also thanks sthe Ohio Supercomputer Center for time on their Cray YMP-8 machine.

Appendix

All calculations have been performed at increasing levels of Moller-Plesset perturbation theory, namely MP2, MP3, and MP4 using Gaussian 92 (Frisch et al. 1992). First, investigations were carried out at the MP2 level using a double-zeta basis set extended by polarization functions (6-31G(d,p)). To obtain accurate electronic energies, single point calculations were performed at the MP4SDTQ/6-311 + + G(3df,3pd) theoretical level using MP2/6-31G(d,p) optimized geometries. These are full fourth order perturbation calculations, including contributions from single, double, triple, and quadruple excitations and employing a triple-zeta basis set extended by polarization and diffuse functions; such basis sets are known to give a large flexibility to the one-particle space approaching the so-called Hartree-Fock limit. The character of each stationary point (either minimum energy, for which all vibrational frequencies are real, or saddle point, characterized by one imaginary frequency) has been confirmed by vibrational analysis at the MP2/6-31G(d,p) theoretical level.

The optimized reaction path considered is C approaching ammonia along its C_{3v} axis. Relative energies have been corrected for zero-point vibrational energy (ZPE) using carefully scaled vibrational wave numbers. The MP2 scaling factor has

been deduced from our previous theoretical study of the HCN, HNC, systems (Talbi et al. 1996). It is equal to 0.969 and has been applied to all molecules studied here.

When indicated, energies have been corrected for spin contamination from higher spin states using an approximate spin projection method, whose description can be found in Schlegel (1986).

Knowing from our past experience that basis set superposition errors (BSSE) (Boys & Bernardi 1970; Liu & McLean 1989) are less than one Kcal/mol (DeFrees et al. 1990, Talbi et al. 1996), they have been neglected in view of the large energy differences involved by the processes studied here.

Since previous theoretical studies (DeFrees & McLean 1985) have shown that calculated rotational constants are much closer to experimental values when third-order perturbation theory is used rather than second-order or fourth-order, the MP3/6-311 + + G(d,p) level has been used for their determination. We have calculated rotational constants for all structures corresponding to either potential minima or saddle points along the lowest potential energy surface leading to $H_2NC^+(^1A_1)$/$HCNH^+$ ($^1\Sigma^+$), since they are required as input for dynamics calculations. For this surface, the final MP4SDTQ calculations have been done using both MP2/6-31G(d,p) and MP3/6-311 + + G(d,p) geometries as a test of energy stability with respect to geometry. A comparison of the MP4SDTQ/6-311 + + G(3df,3pd) calculations obtained using MP2/6-31G(d,p) and MP3/6-311 + + G(d,p) optimized geometries (Table 2) shows energy differences smaller than 0.2 Kcal/mol. These negligible differences justify the use of the MP2/6-31G(d,p) optimized geometries for the $^2A''$ and $^4A''$ surfaces.

References

Allen T.L., Goddard J.D., Schaefer III H.F., 1980, J. Chem. Phys. 73, 3255

Boys S.F., Bernardi F., 1970, Mol. Phys. 19, 553

DeFrees D.J., McLean A.D., 1985, J. Chem. Phys. 82, 333

DeFrees D.J., McLean A.D., Herbst E., 1985, ApJ 293, 236

DeFrees D.J., Binkley J.S., Frisch M.J., McLean A.D., 1986, J. Chem. Phys. 85, 5194

DeFrees D.J., Talbi D., Pauzat F., Koch W. and McLean A.D., 1990, Chemistry and Spectroscopy of Interstellar Molecules. In: Proceedings Pacifichem 89 Symposium, P. 228, Kaifu N ed.

Frisch M.J., Trucks G.W., Head-Gordon M., et al., 1992, Gaussian 92, Revision E. 2, Gaussian, Inc., Pittsburgh, PA

Herbst E., 1982, Chem. Phys. 65, 185

Herbst E., 1996, Gas Phase Reactions. In: Drake G.W.F. (ed.) Atomic, Molecular, & Optical Physics Handbook, Amer. Inst. of Phys., Woodbury, New York, p. 429

Herbst E., Dunbar R.C., 1991, MNRAS 253, 341

Illies A.J., Jarrold M.F., Bass L.M., Bowers M.T., 1983, J. Amer. Chem. Soc. 105, 5775

Irvine W.M., Schloerb F.P., 1984, ApJ 282, 516

Irvine W.M., Goldsmith P.F., Hjalmarson Å, 1987, Chemical Abundances in Molecular Clouds. In: Hollenbach D.J., Thronson, Jr H.A. (eds.) Interstellar Processes, Reidel, Dordrecht, p. 561

Jarrold M.F., Kirchner N.J., Liu S., Bowers M.T., 1986, J. Phys. Chem. 90, 78

Lee H. -H., Bettens R.P. A., Herbst E., 1996, A&AS 119, 111

Liu B., McLean A.D., 1989, J. Chem. Phys. 91, 2348

Marquette J.B., Rowe B.R., Dupeyrat G., Poissant G., Rebrion C., 1985, Chem. Phys. Lett. 122, 431

Millar T.J., Farquhar R.P.A., Willacy K., 1997, A&AS 121, 139

Pineau des Forêts G., Roueff E., Flower D.R., 1990, MNRAS 244, 668

Pratap P., Dickens J.E., Snell R.L., et al., 1997, ApJ, in press

Schlegel H.B., 1986, J. Chem. Phys. 84, 4530

Schilke P, Walmsley M.C., Pineau des Forets G., Roueff E., Flower D.R., Guilloteau S., 1992, A&A, 256, 595

Talbi D., Ellinger Y., Herbst E., 1996, A&A 314, 688

Talbi D., Ellinger Y., 1998, Chem. Phys. Lett, in press

Talbi D., 1998, in preparation

Ungerechts H., Bergin E.A., Goldsmith P.F., et al., 1997, ApJ 482, 245

Watson W.D., 1976, Rev. Mod. Phys. 48, 513

Whitten G.Z., Rabinovitch B.S., 1964, J. Chem. Phys. 41, 1883